Comparison of shear wave velocity measurements in a soft clay specimen using time and frequency domain techniques

David Nash,* Jiraroth Sukolrat,* Paul Greening,** Nadia Benahmed***

Abstract

Bender elements have been used to determine shear wave velocity in specimens of soft Bothkennar clay using two different techniques. Tests have been carried out in a stress-path triaxial cell equipped with bender elements mounted in three orthogonal directions enabling anisotropy of small strain stiffness to be determined. Phase-delay methods have been used to determine travel time in addition to the more common first arrival technique. The phase delay readings show that the soils are dispersive resulting in variations of velocity with frequency. Of much more significance is the finding that the frequency domain method consistently produces an estimate of shear wave velocity which is lower than that from traditional time domain readings. The paper describes observations made as a sample of natural Bothkennar clay was first consolidated to in-situ stress conditions and then destructured by subjecting it to undrained shear. The automated data acquisition system has enabled shear wave velocity determinations by the two methods throughout the test, which provide a useful and unusual data set. The shear wave velocities are compared and the evolving anisotropy is discussed.

Introduction

Bender elements are an increasingly popular tool for determining small strain shear stiffness (G_0) in laboratory soil samples. When an embedded bender element is energised, its movement generates shear waves which result in very small shear strains, estimated by Pennington [1999] to be about 0.0001%. A second embedded bender element located within perhaps 200 mm, may act as a microphone and it generates fluctuating charge which can be observed with a suitable oscilloscope. Numerous researchers (e.g. Viggiani, 1992; Jovičić, 1997) have used bender elements in triaxial apparatus to examine the changes of soils stiffness with soil state; the interpretation of the test data has been discussed, for example, by Viggiani and Atkinson [1995] and Jovičić *et al.* [1996].

The travel time of a pulse disturbance created by a transmitter bender has traditionally been determined from a visual inspection of the highly attenuated trace from a receiver element. It is assumed that the propagated wave is a bulk plane shear wave travelling between source and receiver. While it is sometimes easy to determine first arrival, it is often the cause of much uncertainty. Arroyo [2001] has estimated uncertainties of up to 100% in estimation of the small strain shear stiffness (G_0). The use of continuous signals which require the shear wave velocity to be decoded from measurements of relative phase of transmitted and received signals is gaining in popularity (e.g. Blewett *et al.*, 1999). While the technique is used very widely across a wide range of fields (see for instance Sasche and Pao, 1978), Viggiani and Atkinson [1995] were the first to apply a phase-delay method to bender element testing. These methods have a number of advantages over traditional pulse-based measurements. Chief amongst these is that it is convenient to create an algorithm to determine travel time by establishing the gradient of a graph of phase difference against frequency.

Phase delay methods can be performed reliably using "traditional" equipment i.e. a signal generator and oscilloscope [Kaarsberg, 1975]. A continuous harmonic sinusoid is used as the input signal. The frequency of the signal is changed and the frequencies at which the transmitted signal and received signal are exactly in and out of phase with one another (so called π-points) are noted. Greening and Nash [2004] showed that the same information could be established less onerously using broad-band input signal and a spectrum analyzer. The phase-delay methods applied to bender element readings all reveal a non-linear relationship between relative phase and signal frequency. The factors causing this dispersive relationship continue to be discussed [Rio, 2006]. Given that the relationship applies to the whole system from the transmit-

* Department of Civil Engineering, University of Bristol, U.K.
** Department of Civil and Environmental Engineering, University College London, U.K.
***CEMAGREF Groupement d'Aix en Provence, France (formerly University of Bristol, U.K.)

ted signal through the bender-soil system to the acquired signal there are clearly a number of contenders for the source of dispersion. The characteristics of the electronic part of the system as well as the soil-bender interaction must play a part but so will characteristics of wave motion in the soil such as the near-field effect (see for instance SÁNCHEZ-SALINERO *et al.*, 1986) and wave reflections from sample boundaries. The transfer function of the system, of which the relative phase of the system is a part (along with relative magnitudes of the frequency components), offers a rather complete description of system behaviour. The impulse response function (defined by the inverse Fourier transform of the transfer function) when convolved with any transient input signal (such as traditional pulse signals) will give the resulting received waveform. In the light of this, it seems sensible to determine the transfer-function for these bender-element systems routinely pending further research into how it can be used to establish the true low strain shear stiffness (G_0) of the sample. One possibility is that a numerical model will be used in conjunction with a testing programme with bender element methods used to calibrate the *a priori* model.

This paper describes some observations made as a sample of natural Bothkennar clay was first consolidated to in-situ stress conditions and then destructured by subjecting it to undrained shear. The shear wave velocity determinations by both time domain and frequency domain methods are compared and the evolving anisotropy is discussed. A brief extract of the results described here was included in GREENING *et al*. [2003].

Shear wave velocity measurement using bender elements

Equipment

Bender elements are usually mounted in the platens of a triaxial apparatus and time domain measurements are made to determine the shear wave velocity in the *vh* direction (where *vh* denotes a vertically propagated wave with horizontal polarisation). More recently PENNINGTON [1999] and PENNINGTON *et al.* [2001], mounted bender elements on the sides of a triaxial specimen as well as in the platens, thereby enabling measurements of shear wave velocity in *hv* and *hh* directions in addition to the standard *vh* direction. This arrangement was used in the present research. The platen-mounted bender elements used in the triaxial cells are 10 mm wide by 10 mm high protruding several millimetres through the porous discs into the soil. The lateral benders are mounted in small pots embedded several millimetres in the triaxial specimens, and are 5 mm wide by 4 mm long. The pots are held in place by a rubber grommet, similar to that used to mount a mid-height pore pressure transducer. In this research specimens were generally 150 mm high by 75 mm diameter, and the arrangement of bender elements was as shown in Figure 1.

Traditionally a function generator is used to generate a pulse and both the transmitted and the received waves are displayed on an oscilloscope. In the test programme described here such an arrangement was used initially with a TG1010 function generator providing a sine pulse with a frequency of 5 kHz, -90° phase shift and an amplitude of 20 Vpp.

In parallel with this research on Bothkennar clay, research was being carried out on synthetic samples by RIO [2006] using phase delay methods explored by GREENING and NASH [2004]. For the frequency domain measurements a sound card installed in a PC was used to generate a series of sine sweep pulses, and a Pico Technology ADC216 was used for high speed data acquisition. The amplitude of the signal produced by an in-built sound card is typically around +/- 2.5V. The maximum sampling

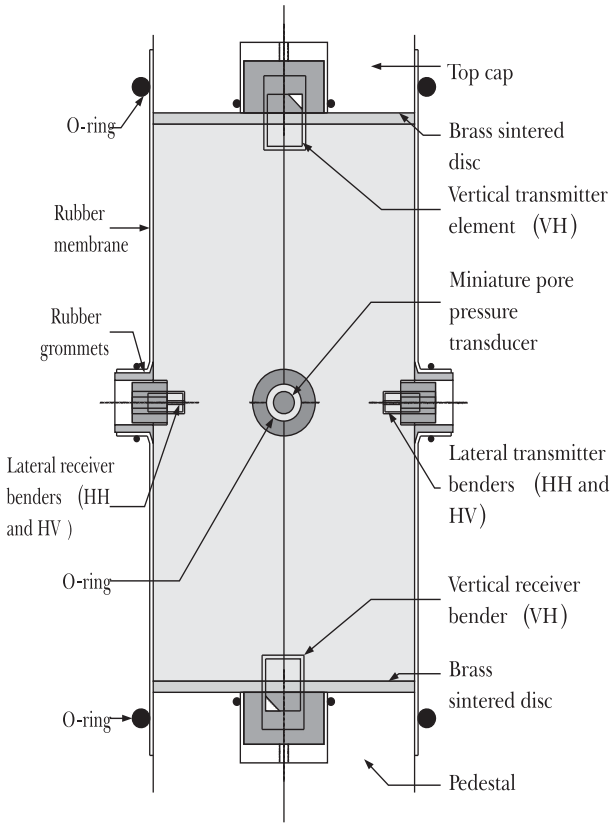

Fig. 1 – Bender element mountings for *vh*, *hv* and *hh* directions.
Fig. 1 – Installazione del bender element per le direzioni vh, hv e hh.

frequency of the sound card (typically around 50kHz) places a limitation on the resolution with which the first rise of a transient signal can be generated. Best results have been obtained with a swept-sine signal with a 0 to 20kHz bandwidth. This signal has been found to be sufficient to establish the transfer function arising between this signal and the received signal. A PC based system was developed to perform a transfer function estimate and to determine the travel times for bender element systems [GREENING, 2005]. This automatic bender element testing system (ABETS) is effectively a low-cost spectrum analyser and was implemented in Microsoft Excel™.

It was found from experience that the sound card could also be used to generate the sine pulse with little loss of accuracy, and this led to development of a multiplex system for automatic collection of bender reading data. The data acquisition system can use the same computer that controls the stress-path triaxial test to generate the pulses, collect the data, and switch between the various directions as shown schematically in Figure 2. All data are saved on the computer for subsequent manual interpretation.

Time domain method

At the start of the research, pilot tests were carried out on a specimen of reconstituted Bothkennar clay (specimen BR4) to compare velocity measurements made using various techniques. The 75 mm diameter by 150 mm high sample was K_0 consolidated from slurry under 150 kPa vertical stress and allowed to swell back to q = 40 kPa and p' = 53 kPa when tests were carried out. For the tests using traditional time domain methods, three pulse signals were propagated in each of the three measurement directions as shown in Figure 3; all three were based on a sine wave of frequency 5 kHz. The asymmetrical pulse signal (VJ) was suggested by JOVIČIĆ [1997] to mitigate the near field effects which tend to obscure a clear first arrival. Several points could be taken to indicate the first arrival of the received signal, including the first deviation from zero, the first inversion point, the first crossing point, or the first peak of the signal [BRIGNOLI *et al.*, 1996]. Throughout the research, the signal received from horizontally propagated waves (*hh* and *hv*) generally showed an abrupt deviation from zero, so it was straightforward to define the point of first arrival. In the vertical direction (*vh*), near field effects resulted in an initial negative deviation of the signal so the point of arrival was taken as the first inversion of the signal. The figure shows the (normalised) transmitted and received signals and indicates very similar points of first arrival for all three waves; the arrows labelled TD indicate the first arrival positions chosen. The velocities corresponding to these travel times are given in Table I.

It was also found that due to near field effects, the observed travel time was influenced by the exci-

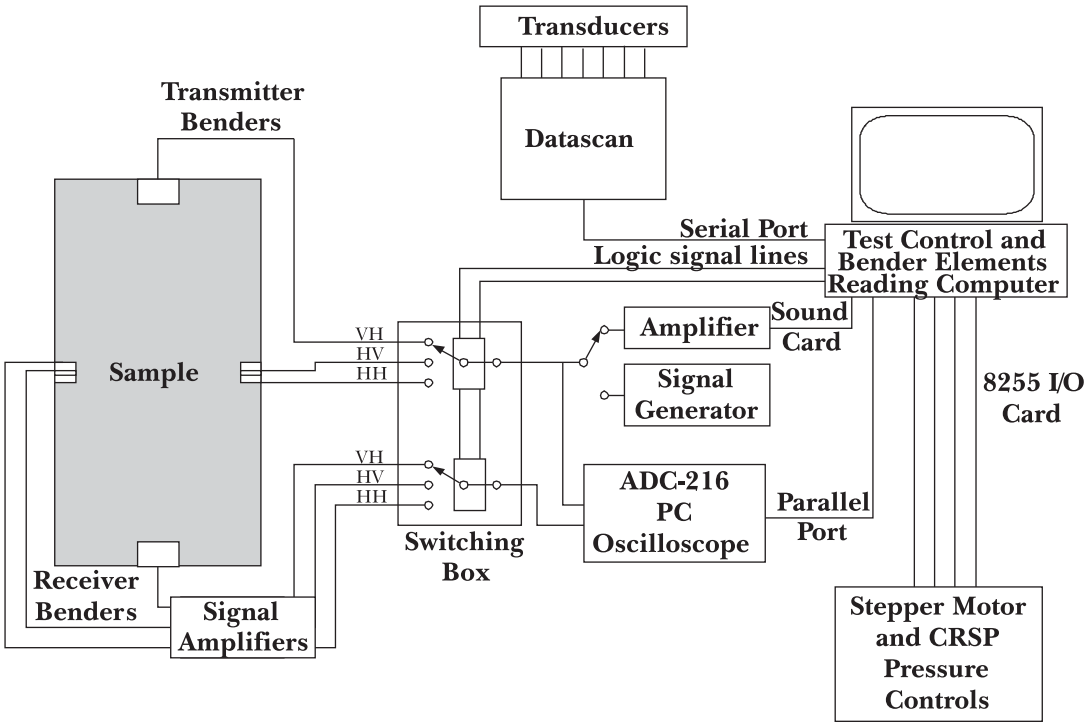

Fig. 2 – Schematic diagram of bender data acquisition system.
Fig. 2 – Schema del sistema di acquisizione dati del bender element.

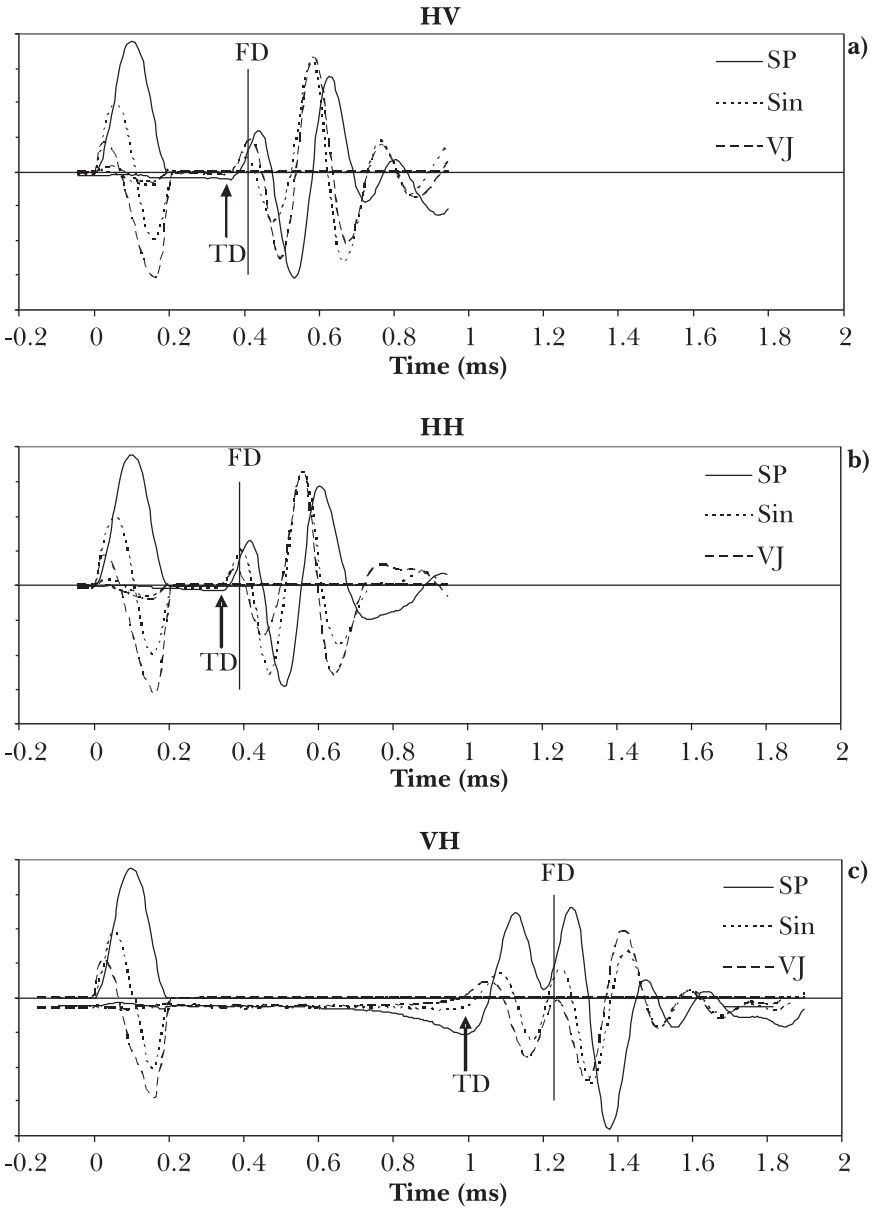

Fig. 3 – Pulse readings on reconstituted sample of Bothkennar clay: "normalised voltages" for a) *hv* b) *hh* and c) *vh* directions.
Fig. 3 – Letture sul campione ricostituito di argilla di Bothkennar per le direzioni a) hv, b) hh e c) vh.
Note:Le frecce marcate con TD indicano i punti di primo arrivo; le linee verticali marcate con FD indicano i punti di arrivo calcolati dalle prove nel dominio della frequenza.

Tab. I – Comparative Vs measurements on specimen BR4.
Tab. I – Confronto tra le misurazioni di V_s sul provino BR4.

	Shear wave velocity (m/sec)		
	hv	hh	vh
Pulse (TD)	158	169	134
Phase-delay (FD)	138	145	108

tation pulse frequency, but careful tests showed that selection of a 5kHz pulse resulted in representative and consistent data. At this frequency, the ratio of path length to wavelength R_d was typically about 2 in the horizontal direction and 5 in the vertical direction.

After these pilot tests it was decided to use a pulse based on a 5 kHz sine wave with -90° phase shift (type SP in Fig. 3) as a standard. Such a wave can be generated by the sound card with little loss of accuracy since there are no sudden deviations in the signal. The wave velocity was calculated assuming a path length equal to the current distance between the tips of the bender elements.

Frequency domain methods

After determinations of shear wave velocity using the time domain technique, the same specimen was used for frequency domain measurements. First the phase component of the transfer function was

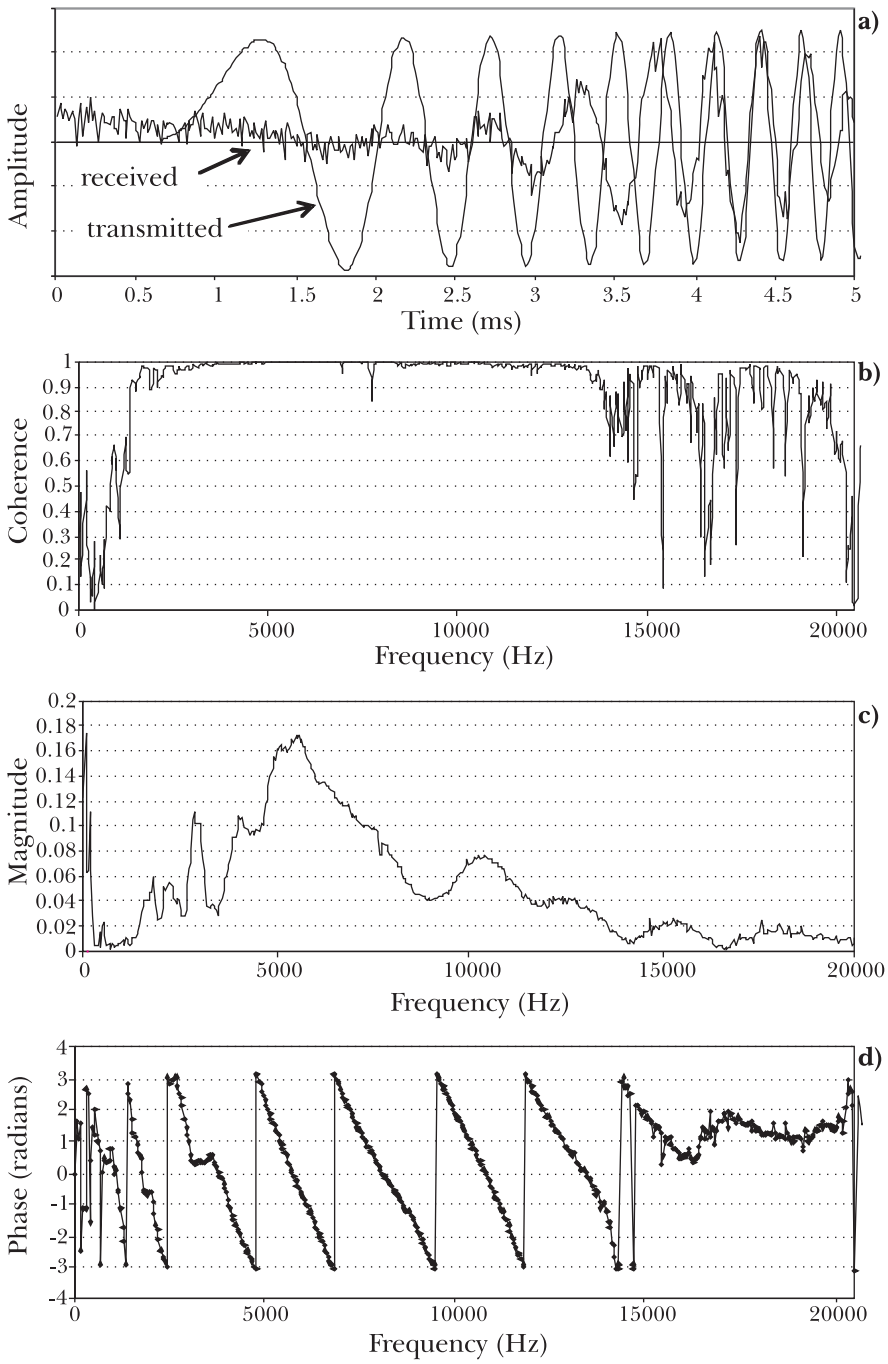

Fig. 4 – a) start of frequency-sweep signal, b) coherence, c) magnitude and d) phase for system transfer function (Test BR4 *hv* direction).

Fig. 4 – a) inizio del segnale di scansione in frequenza, b) coerenza tra input e output, c) ampiezza e d) fase della funzione di trasferimento del sistema (test BR4, direzione hv).

determined using the π-point method, and then the complete transfer function was established using the ABETS testing system described above. The top plot in Figure 4 shows the start of the transmitted frequency sweep signal as well as the first arrival of the signal. The other graphs show the relative phase between the two signals and the magnitude of the transfer function for one of the propagation paths (*hv*), together with the coherence function between the transmitted and received signal (an indication of the correlation of the two signals). The phase relationship is clearly reasonably well defined in the region 2 to 14 kHz. There are some fairly distinct system resonances between approximately 1 and 4 kHz which result in some local phase-shifts. Frequency ranges giving coherence values close to unity give confidence that the estimate of transfer function in that region is not corrupted by noise.

The phase relationship defined between $-\pi$ and π was unwrapped to find the total phase difference

between transmitted and received signals. Given the poor definition of the transfer function in the low frequency range, the absolute phase is difficult to establish. Figure 5 shows the unwrapped phase plotted on top of the π-point measurements. There is a good agreement giving confidence in the transfer-function estimation routine. The low-frequency divergence for the *hv* signal may result from the unwrapping algorithm. Any differences could also result from the fact that the measurements are taken with different electronics.

The group travel time t_{gr} [GREENING and NASH, 2004] may be determined from the average slope of the unwrapped phase relationship by:

$$t_{gr}=\frac{1}{2\pi}\frac{d\varphi}{df}$$

where φ is the phase angle and f is the frequency. For the *hv* direction shown in Figure 4 a best-fit line was fitted to the unwrapped data in Figure 5 over the user-specified frequency range from 4 to 13 kHz, and a similar procedure was followed for the other directions. The calculated travel times are given in Table I and are indicated on Figure 3 by vertical lines labelled FD. It may be seen that for each direction, the inferred travel time is longer than that calculated from the time domain measurements. The group velocities were obtained using the distance between the tips of the benders and are compared with the time domain data. In all three directions the frequency domain measurements indicate a lower shear wave velocity (and hence G_0 value) than the more traditional pulse technique.

Observations of shear wave velocity in a natural soft clay sample

Sample tested

The test BN10 described in this paper was one of several designed to explore the changes of shear modulus G_0 resulting from controlled destructuration of Bothkennar clay, an estuarine clayey silt / silty clay of high plasticity. Bothkennar clay [NASH *et al.*, 1992] was chosen because of the availability of some high quality natural soil samples, obtained using the Sherbrooke sampler [LEFEBVRE and POULIN, 1979] in 1997. These samples were found to be in good condition despite having been stored for more than 5 years. At Bothkennar, there are different facies with distinct properties [PAUL *et al.*, 1992; CLAYTON *et al.*, 1992], but all the samples tested were from the mottled facies with the majority of samples (including specimen BN10) taken from around 8.0 m depth. Bothkennar clay is an estuarine or shallow marine silty clay / clayey silt deposit and at this depth it is believed to have been bioturbated after deposition [PAUL *et al.*, 1992] as indicated by the mottling. The clay is significantly structured with a

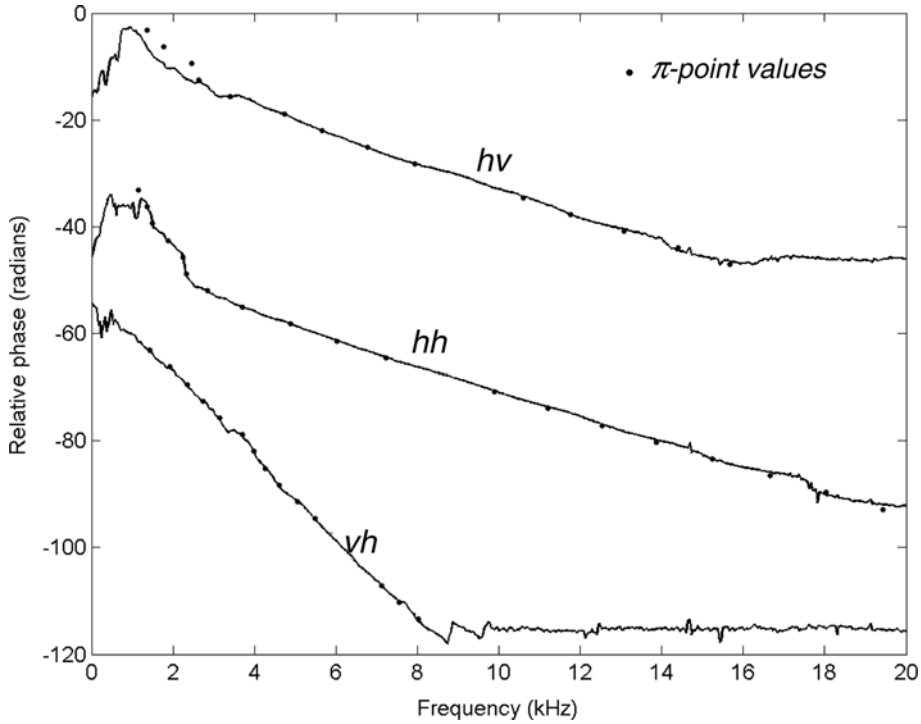

Fig. 5 – Unwrapped phase compared with π-point measurements.
Fig. 5 – Confronto tra le curve fase relativa-frequenza e dai relativi ai punti π.

Tab. II – Typical properties of natural Bothkennar clay from 8.0 m depth.
Tab. II – Proprietà dell'argilla naturale di Bothkennar a 8 m di profondità.

Water content (%)	72%
Liquid limit, w_L (%)	79%
Plastic limit, w_P (%)	37%
Activity	1.34
Organic matter (%)	5%
Undrained strength (kPa)	25 kPa
OCR	1.6

void index[1] of about 1.0. Each Sherbrooke sample was carefully divided and trimmed using a wire saw into several specimens of natural clay. Specimen BN10 was initially 75 mm diameter by 150 mm high. Typical properties of the clay from that depth are given in Table II. Full details of the test equipment and test programme are given by SUKOLRAT [2007].

Stress-strain path followed

Details of the imposed stress and strain paths are shown in Figure 6. The initial suction in the specimen was estimated to be approximately 20 kPa, so this value was applied as an initial cell pressure and was used throughout the test as a reference stress (point I in Fig. 6a). The specimen was then reconsolidated under the estimated in-situ stresses (K_0 = 0.65: point A in Fig. 6a) before being subjected to an undrained compression-extension loop with a strain amplitude of ±2%. The strain path followed in the compression-extension loop was intended to be similar to that thought to be applied to an element at the centre-line of a sample during tube-sampling of soft clays [BALIGH, 1985; BALIGH *et al.*, 1987; CLAYTON *et al.*, 1992]. This was followed by a return to the isotropic stress state, and after further recompression back to the in-situ stress state (which was accompanied by reduction of volume), the sample was sheared undrained to failure. Again the sample was returned to the isotropic stress state, followed by recompression back to the in-situ stress state before finally unloading back to the isotropic state. At each stage the stresses were held constant until the axial creep rate reduced to less than 0.01%/day, before bender element readings were taken.

Shear wave velocity determinations

At various stages during the test, shear wave velocity measurements were made using both time domain and frequency domain techniques. The automated reading system enabled measurements to be taken at prescribed intervals, although in this test a full set of readings was only taken in the *vh* direction as the multiplex switch was still under development. For the other directions data have been interpo-

[1] To quantify the structure of a natural clay, BURLAND [1990] introduced the term void index $I_v = \frac{e_0 - e^*_{100}}{e^*_{100} - e^*_{1000}}$ where e_0 is the void ratio of the natural clay in-situ, and e^*_{100} and e^*_{1000} are the void ratios of the reconstituted clay consolidated in the oedometer under 100 and 1000 kPa respectively.

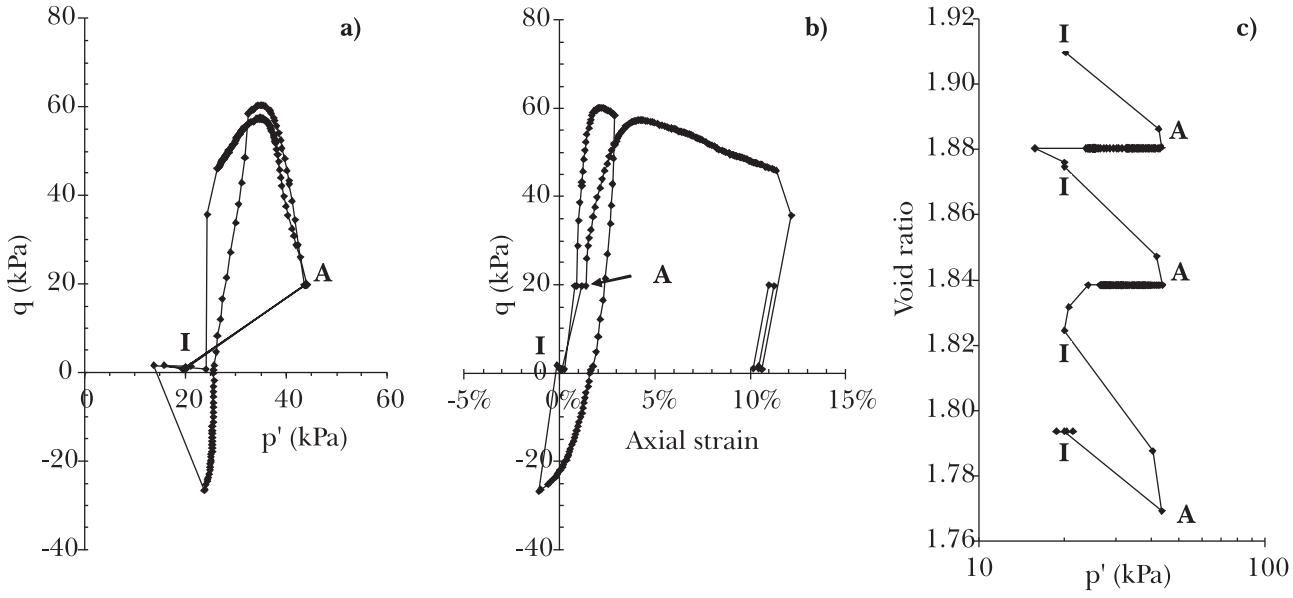

Fig. 6 – a) q vs p stress path, b) q vs axial strain and c) void ratio vs p in Test BN10.
Fig. 6 – a) percorso q-p', b) andamento di q con la deformazione assiale, c) andamento dell'indice dei vuoti con p' nella prova BN10.

lated as indicated by the dotted lines on the graphs. The velocity was determined assuming a path length equal to the current tip-to-tip distance between the pair of bender elements in use. The variation of these velocities throughout the test is plotted in Figure 7 against cumulative axial strain together with the variation of the deviator stress. Cumulative axial strain (with all strain increments taken as positive) is used rather than elapsed time for clarity. The isotropic and in-situ stress states are labelled I and A respectively; velocities and velocity ratios determined at these states are given in Table III.

The shear wave velocities varied throughout the tests as a result of changes of stress, volume changes and damage to the clay structure. It may be seen that in each direction the two values of velocity were different, with that obtained from first arrival of the pulses (time domain technique) always faster than that obtained using the frequency domain method. However it is apparent that the same trends affect both types of measurement.

The data at several stages of the test are discussed below.

UNDER ISOTROPIC STRESS CONDITIONS

At the start of the test, when the specimen was set first up and the bender elements embedded in the unconfined sample, the velocities in all three directions were very similar at around 87 m/sec (time domain) and 77 m/sec (frequency domain). Once the cell had been filled with pressurised water and back-pressure applied giving an isotropic effective stress of 20 kPa (state I), the velocities in all three directions had increased to around 95 m/sec (time domain TD) and 82 m/sec (frequency domain FD). This isotropic behaviour reflects the fabric of the natural material which as noted above, is believed have been bioturbated post-deposition. The changes of velocity during initial consolidation and the 15% difference between the two sets of velocity measurements (TD and FD) was also observed in other tests in the research.

AFTER RECONSOLIDATION UNDER IN-SITU STRESSES

Consolidation of the specimen under the in-situ stresses (point A) further increased the shear wave velocities to average 109 m/sec (TD) and 90 m/sec (FD). At this stage of the test there had been less than 1% volume change (or $\Delta e/e_0$ of less than 0.02) which is confirmation of the very high quality of this Sherbrooke sample (see for example LUNNE *et al.*, 1997). These velocities may be compared with in-situ cross-hole geophysics measurements at 8.0m depth at Bothkennar that ranged from 110 m/sec to 125 m/sec (*hh* and *hv* directions respectively, HOPE *et al.*, 1999). The in-situ measurements of the shear wave velocity indicate an anisotropy ratio V_{shh}/V_{shv} of 0.88 whereas the laboratory values of velocity are equal.

CHANGES DURING UNDRAINED STRESS-STRAIN EXCURSION

The undrained shear excursion (±2% axial strain) reduced the shear wave velocity in all three directions, partly as a result of the changing effective stress, but more importantly as a result of the damage to the clay structure induced by undrained shear strains. Peak strength occurred after 1% axial strain (see Fig. 6), but velocities decreased immediately on loading due to the reduction of effective stresses (see Fig. 7). The change of strain direction from compression to extension is followed by further reductions in velocities (V_{shv} and V_{svh}) associated with the reduction of vertical effective stress. The velocity V_{shh} increased somewhat during the extension stage as a consequence of the increase of horizontal effective stress. By the end of the loop, under isotropic stresses before re-consolidation, the velocities had reduced by 15 to 25% from the values under in-situ stress (point A). Figure 7 shows that for each direction (*vh*, *hv*, *hh*) the trends of two measurements of shear-wave velocity (TD and FD) were broadly similar, but in each case the frequency domain measurements yielded lower velocities.

AFTER RECONSOLIDATION UNDER IN-SITU STRESSES

Reconsolidation of the specimen, firstly under isotropic stresses of 20 kPa (point I) and then under in-situ stresses (point A) was accompanied by a small (1.5%) volume reduction (see Fig. 6c). Together with the increase of effective stress this resulted in an increase in the shear wave velocities so that they were very similar (96%-102%) to those measured under in-situ stresses initially (see Fig. 7). Despite the damage to the clay structure caused by the undrained loop, its effect is masked by the effects of the volume changes. To reveal the effects of destructuration it is necessary to normalise the data to take account of the volume changes – which will not be discussed further in this paper.

CHANGES DURING UNDRAINED COMPRESSION TO FAILURE

After maintaining the stresses constant at the in-situ stress state (point A), the sample was then sheared in undrained compression to 10% axial strain. Figure 6a indicates that the stress path followed was very similar to that of the first part of the previous undrained shear loop. It may be seen from the stress-strain curve shown in Figure 6b, that the previous undrained loop had little effect on the subsequent undrained strength probably because the damage to the clay structure was offset by the volu-

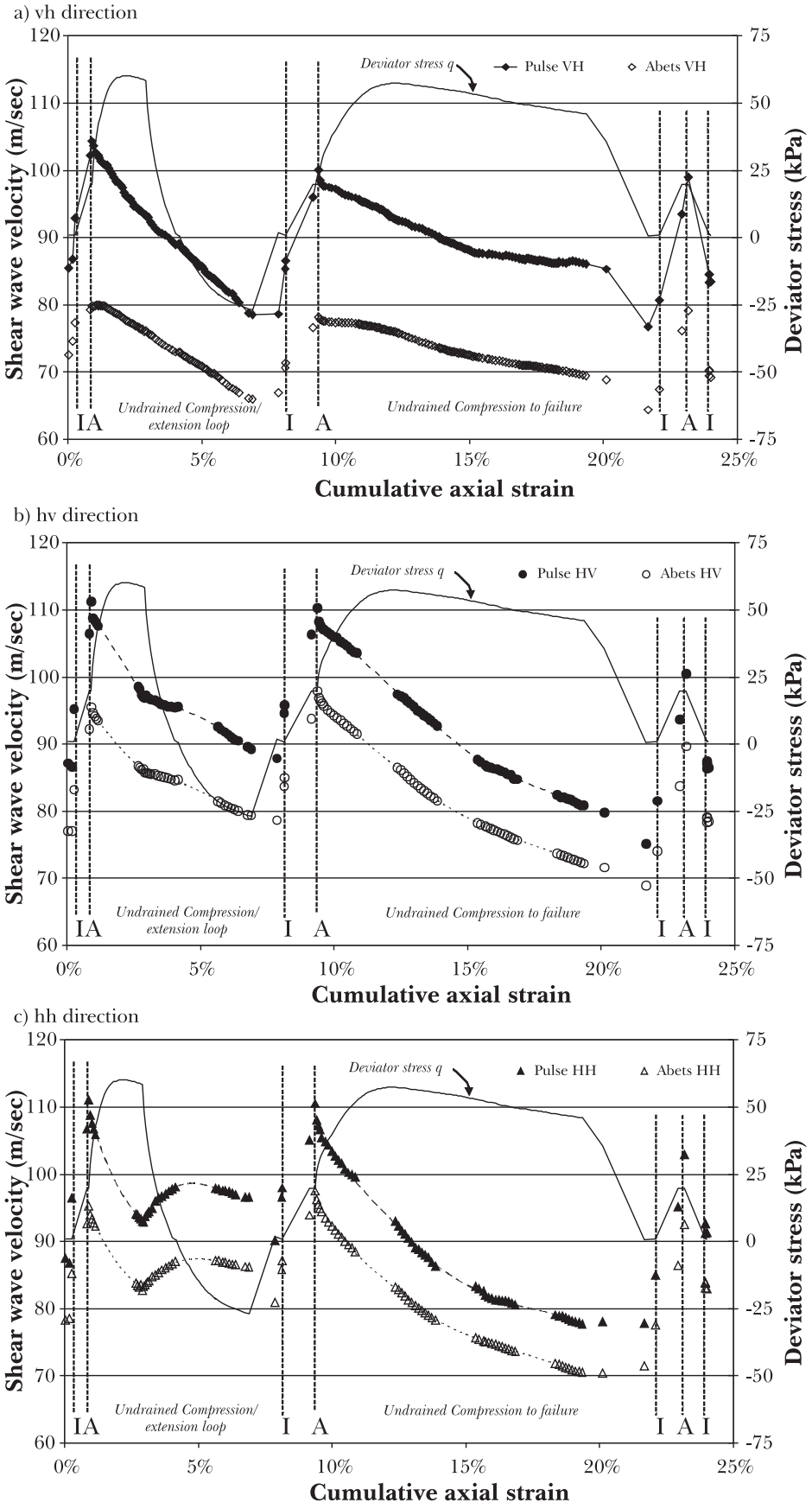

Fig. 7 – Variation of shear wave velocities and deviator stress during test BN10 in a) vh direction, B) hv direction, and c) hh direction.

Fig. 7 – Variazione delle velocità delle onde di taglio e dello sforzo deviatorico durante il test BN10 nelle direzioni a) vh, b) hv, c) hh.

Tab. III – Comparative Vs measurements on specimen BN10.
Tab. III – Confronto tra le misurazioni di V_s sul provino BN10.

State	Pulse (TD) shear wave velocities (m/sec)			Abets (FD) shear wave velocities (m/sec)			Ratios Pulse/Abets TD/FD			Anisotropy ratios			
	vh	hv	hh	vh	hv	hh	vh	hv	hh	hh/hv TD	hh/hv FD	vh/hv TD	vh/hv FD
In air	85.5	87.2	92.6	70.2	79.1	83.9	1.20	1.10	1.10	1.06	1.06	0.97	0.89
I	92.9	95.3	96.5	77.3	83.3	85.3	1.20	1.14	1.13	1.01	1.02	0.98	0.93
A	104.3	111.3	111.1	79.9	95.6	95.3	1.31	1.16	1.17	1.00	1.00	0.94	0.84
Undrained compression-extension loop													
I	86.6	95.8	98.0	71.4	85.0	87.2	1.21	1.13	1.12	1.02	1.02	0.90	0.84
A	100.1	110.3	110.5	78.1	98.0	97.5	1.28	1.13	1.13	1.00	1.00	0.91	0.80
Undrained shear to 10% axial strain													
q=0	76.7	75.2	77.9	64.4	69.0	71.5	1.19	1.09	1.09	1.04	1.04	1.02	0.93
I	80.7	81.6	85.0	67.4	74.1	77.6	1.20	1.10	1.10	1.04	1.05	0.99	0.91
A	99.0	100.5	102.9	79.2	89.7	92.5	1.25	1.12	1.11	1.02	1.03	0.99	0.88
I	84.5	87.1	92.6	70.2	79.1	83.9	1.20	1.10	1.10	1.06	1.06	0.97	0.89

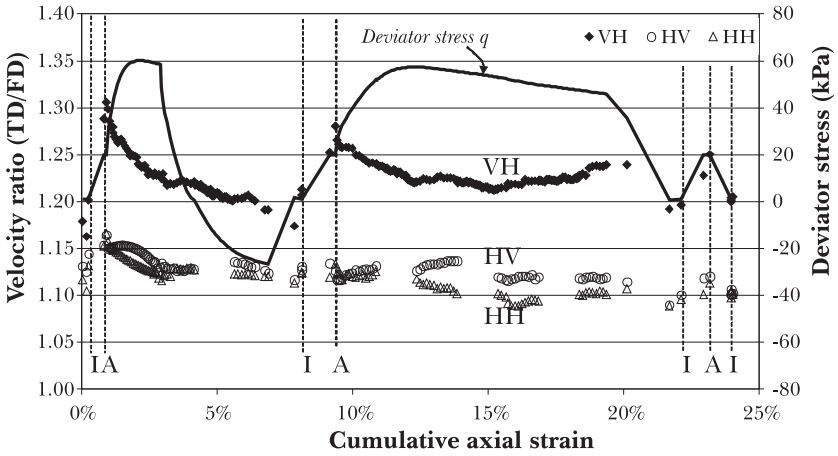

Fig. 8 – Variation of velocity ratios comparing time domain (TD) and frequency domain (FD) through test BN10.
Fig. 8 – Variazione dei rapporti di velocità durante il test BN10; confronto tra il dominio del tempo (TD) e della frequenza (FD).

metric hardening. As was noted above the shear wave velocities (and hence G_0) had recovered under in-situ stresses (point A), but Figure 6b shows that the medium strain stiffness was noticeably reduced from that in the previous loop.

The shear velocities again reduced during the undrained shear stage from averages of 107 m/sec (TD) and 91 m/sec (FD) initially, by 20 to 30% to averages of 77 m/sec (TD) and 68 m/sec (FD) at the end of the stage. The proportionate reduction of the two pairs of velocity measurements for the horizontally propagated waves was very similar at about 30% with that of the vertically propagated waves rather smaller.

FURTHER CHANGES AFTER FINAL RECONSOLIDATION

At the end of undrained compression the deviator stress was removed and the specimen was again re-consolidated firstly under isotropic stresses of 20 kPa (point I) and then under in-situ stresses (point A). This was accompanied by a further small (2.5%) volume reduction (see Fig. 6c). Together with the increase of effective stress this resulted in an increase in the shear wave velocities so that they were still very similar to those measured under in-situ stresses initially (see Figure 7). Thus under in-situ stress, the velocities averaged 101 m/sec (TD) and 87 m/sec (FD) at the end of the test, compared with averages of 109 m/sec (TD) and 90 m/sec (FD) initially, changes of 93% and 97% respectively.

Ratio between time domain and frequency domain measurements

Figure 7 shows that for each direction (*vh*, *hv*, *hh*) the trends of the two measurements of shear-wave velocity (TD and FD) were broadly similar, but in each

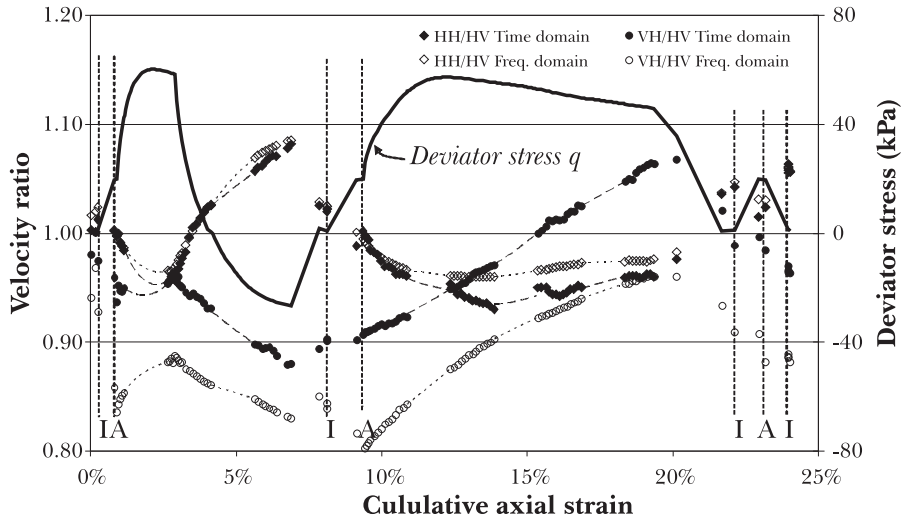

Fig. 9 – Variation of anisotropy of shear wave velocity comparing time domain and frequency domain through test BN10.
Fig. 9 – Variazione dell'anisotropia della velocità delle onde di taglio durante il test BN10; confronto tra il dominio del tempo e della frequenza.

case the frequency domain measurements yielded slower velocities. The ratios between the pairs of velocities determined using time domain and frequency domain (TD/FD) for each direction (*vh*, *hv*, *hh*) are shown in Figure 8. It is noticeable that the ratios for the two sets of velocities taken with horizontally propagated waves were very similar throughout the test and only varied from 1.16 initially (under in-situ stresses), to 1.10 at the end of the test despite the significant reductions of velocity at various stages. The ratio for the vertically propagated waves reduced from about 1.3 at the start to 1.2 at the end of the test, and close examination of the data indicates that this ratio is influenced by stress ratio.

It is suspected that the measured velocities are influenced by sample shape and proximity of the boundaries, and that the waves are not in fact pure bulk shear waves. Analytical studies by ARROYO *et al.* [2006] have shown that differences between the two measurements for vertically propagated waves may be caused by the test conditions such as wave reflections from the lateral surfaces as well as end effects. It appears that such effects are smaller for the mid-height (*hv*, *hh*) benders than for the platen-mounted pair (*vh*), and the observed responses are more self-consistent for the horizontal propagated waves than for the vertical waves.

Changes in anisotropy

The anisotropy of the shear wave velocity in a natural clay soil is influenced by the fabric, the micro-structure and by the applied stresses. The fabric of the clay may give rise to anisotropy both at a macro-level due to layering within the soil and at a microscopic level (for example due to preferred orientation of particles). The structure of the clay is affected by post-depositional processes such as creep, thixotropy, cementation, and diagenesis. Bothkennar clay is known to be structured, since the natural clay exists at void ratios that are outside the state boundary surface for the same clay when reconstituted. However as noted above there was post-depositional bioturbation of the clay at this depth which removed obvious layering.

The anisotropy of shear wave velocity is presented in Figure 9 where the ratios of V_{shh}/V_{shv} and V_{svh}/V_{shv} are plotted for both the time domain and frequency measurements. The data show that the anisotropy ratios V_{shh}/V_{shv} determined from the two sets of measurements (TD and FD) using the horizontally propagated waves are very similar throughout the test while the two sets of ratios V_{svh}/V_{shv} comparing vertically and horizontally propagated waves are quite different. Theoretically for an elastic material $V_{svh} = V_{shv}$, but the data from this test do not show this.

It is useful to distinguish initial anisotropy of a sample from changes in anisotropy induced by subsequent changes of stress and strain. The initial anisotropy of this sample V_{shh}/V_{shv} was determined at the initial isotropic stress state (state I) and was found to be minimal. Examining the ratio V_{shh}/V_{shv} determined subsequently under isotropic stresses, this ratio increased very slightly through the test to 1.05 by the end. This small anisotropy is consistent with the fact that the material is a clayey silt / silty clay and electron micrographs reveal a low proportion of platey particles. This ratio is similar to that observed in the tests on reconstituted Bothkennar clay sample BR4 (see Tab. I), but smaller than that observed in some other reconstituted Bothkennar clay samples (1.0 to 1.6 depending on the void ratio), and considerably smaller than the anisotropy ratios of 1.5 to 1.9 observed in specimens of recon-

stituted Gault clay [NASH *et al.,* 1999] which contain a higher proportion of platey clay particles.

The changes in anisotropy during the test are consistent with the application of anisotropic effective stresses. It is well established that the shear wave velocity is primarily influenced by the stresses in the plane of wave propagation.

Conclusions

The automated bender element testing system used in this research has enabled measurements of shear wave velocity to be obtained at regular intervals during a test using both time domain and frequency domain techniques. This has provided a useful and rare data set allowing comparison between the two methods in the three orthogonal directions. The transfer function determined using the phase-delay method provides a complete description of the dynamic system that is convenient for post-processing; the stored data are available for future back analysis.

The data have revealed that shear wave velocities determined by the two methods are related but different. For waves propagated horizontally (*hv* and *hh*) the ratio of the TD to the FD velocities remained constant throughout the test despite the sample reaching failure in compression and extension, with the TD velocity always 10 to 15% greater than the FD velocity. The difference probably arises because the transmitted wave is not a pure plane shear wave, but contains components which travel faster and obscure the arrival of the true shear wave front. In the vertical propagation direction *vh* the difference varied between 17 and 32% during the test. This more pronounced difference is believed to result from the effects of the rigid boundaries at the platens and wave reflections off the sides of the specimen [ARROYO *et al.*, 2006], which perhaps are influenced by the changing specimen shape as the sample experiences first compression and then extension.

These differences between velocities determined using time domain and frequency domain techniques have clear implications for the determination of small strain shear stiffness G_0. The observed 30% difference in TD and FD velocities implies that if conventional TD bender elements measurements are made in the *vh* direction, G_0 may be overestimated by a factor of 2, although it may also be noted that the TD velocities are close to the values from in-situ geophysics. The reasons for the differences are the subject of ongoing research.

The anisotropy of this specimen determined from *hv* and *hh* velocities was small and was very consistent between the two types of measurement. Significant differences between *vh* and *hv* velocities measured on a single sample have been observed previously in research at Bristol and elsewhere. In contrast, JOVIČIĆ and COOP [1998] measured similar *vh* and *hv* velocities using waves propagated axially through cylindrical specimens of natural and reconstituted London clay that had been cut vertically and horizontally. As noted above, theoretically in a homogeneous transverse isotropic elastic medium the two velocities should be the same providing the vertical axis of wave propagation coincides with the axis of symmetry, as discussed by ARROYO and MUIR WOOD [2004]. In layered soils it is expected that the two velocities would be different but the sample tested here was not visibly layered. Rather the differences appear to relate to boundary effects that particularly affect the *vh* velocity measurements. The evidence presented here suggests that waves propagated horizontally through triaxial specimens provide more robust determinations than those propagated vertically.

Acknowledgements

The authors gratefully acknowledge the support of the laboratory staff Mike Pope, Steve Iles and Mark Fitzgerald. The research was partly funded by the UK Engineering and Physical Sciences Research Council.

References

ARROYO M. (2001) – *Pulse tests in soil samples*. PhD Thesis, University of Bristol.

ARROYO M., MUIR WOOD D. (2004) – *Discussion: On the applicability of cross-anisotropic elasticity to granular materials at very small strains*. Géotechnique, 54, n. 1, pp. 75-76.

ARROYO M., MUIR WOOD D., GREENING P. D., MEDINA L., RIO J. (2006) – *Effects of sample size on bender-based axial G_0 measurements*. Géotechnique, 56, n. 1, pp. 39-52.

BALIGH M.M. (1985) – *Strain path method*. J. Geotech. Eng. Div., ASCE. 111, GT9, pp. 1108-1136.

BALIGH M.M., AZZOUZ A.S., CHIN C.T. (1987) – *Disturbance due to ideal tube sampling*. J. Geotech. Eng. Div., ASCE. 113, GT7, pp. 739-757.

BLEWETT J., BLEWETT I.J., WOODWARD P.K. (1999) – *Measurement of shear wave velocity using phase sensitive detection techniques*. Canadian Geotechnical Journal, 36, pp. 934-939.

BRIGNOLI E.G.M., GOTTI M., STOKOE, K.H.II. (1996) – *Measurement of shear waves in laboratory specimens by means of piezoelectric transducers*. Geotech. Test. J., 19, n. 4, pp. 384-397.

BURLAND J.B. (1990) – *On the compressibility and shear strength of natural clays*. Géotechnique, 40, n. 3, pp. 329-378.

CLAYTON C.R.I., HIGHT D.W. and HOPPER R.J. (1992) – *Progressive destructuring of Bothkennar clay: impli-*

cations for sampling and reconsolidation procedures. Géotechnique, 42, n. 2, pp. 219-240.

GREENING P.D. (2005) – *Automatic Bender Element Testing System* (ABETS). http://www.ci-veng.ucl.ac.uk/abets/.

GREENING P.D., NASH D.F.T., BENAHMED N., FERREIRA C., VIANA DA FONSECA A. (2003) – *Comparison of shear wave velocity in different materials using time and frequency domain techniques.* Lyon'03 International symposium on deformation behaviour of geomaterials (Eds. H. DI BENEDETTO, T. DOANH, H. GEOFFROY and C. SAUZEAT), Balkema, Rotterdam, pp. 381-386.

GREENING P.D., NASH D.F.T. (2004) – *Frequency domain determination of G_0.* ASTM Geotechnical Testing Journal, 27, n. 3, pp. 288-294.

HOPE V.S., CLAYTON C.R.I., BUTCHER A.P. (1999) – *In situ determination of G(hh) at Bothkennar using a novel seismic method*. Quarterly Journal Of Engineering Geology, 32, n. 2, pp. 97-105.

JOVIČIĆ V. (1997) – *The measurement and interpretation of small strain stiffness of soils.* PhD Thesis, Department of Civil Engineering, City University.

JOVIČIĆ V., COOP M.R., SIMIC M. (1996) – *Objective criteria for determining G_{max} from bender element tests.* Géotechnique, 46, n. 2, pp. 357-362.

JOVIČIĆ V., COOP M.R. (1998) – *The measurement of stiffness anisotropy in clays with bender element tests in the triaxial apparatus.* ASTM, Geotechnical Testing Journal, 21, n. 1, pp. 3-10.

KAARSBERG E.A. (1975) – *Elastic-wave velocity measurements in rocks and other materials by phase-delay methods.* Geophysics, 40, pp. 955-901.

LEFEBVRE G., POULIN C. (1979) – *A new method of sampling in sensitive clay*. Canadian Geotechnical Journal, 16, n. 1, pp. 226-233.

LUNNE T., BERRE T., STRANDVIK S. (1997) – *Sample disturbance effects in soft low plastic Norwegian clay.* In Recent Developments in Soils and Pavement Mechanics, (Ed. Almeida), Balkema, Rotterdam, pp. 81-102.

NASH D.F.T., LINGS M.L., PENNINGTON D.S. (1999) – *The dependence of anisotropic G_0 shear moduli on void ratio and stress state for reconstituted Gault clay.* In: Prefailure Deformation Characteristics of Geomaterials (Ed. Jamiolkowski *et al.),* Balkema, Rotterdam, pp. 229-238.

NASH D.F.T., POWELL J.J.M., LLOYD I.M. (1992) – *Initial investigations of the soft clay test site at Bothkennar.* Géotechnique, 42, n. 2, pp. 163-181.

PAUL M.A., PEACOCK J.D., WOOD B.F. (1992) – *The engineering geology of the Carse clay at National Soft Clay Research site, Bothkennar*. Géotechnique, 42, n. 2, pp. 183-198.

PENNINGTON D.S. (1999) – *The anisotropic small strain stiffness of Cambridge Gault clay*. PhD Thesis, University of Bristol.

PENNINGTON D.S., NASH D.F.T., LINGS M.L. (2001) – *Horizontally mounted bender elements for measuring anisotropic shear moduli in triaxial clay specimens*. Geotechnical Testing Journal, 24, n. 2, pp. 133-144.

RIO J. (2006) – *Advances in laboratory geophysics using bender elements.* PhD Thesis, University of London.

SACHSE W., PAO Y.-H. (1978) – *On the determination of phase and group velocities of dispersive waves in solids.* Journal of Applied Physics, 49, n. 8, pp. 4320-4327.

SÁNCHEZ-SALINERO I., ROESSET J.M., STOKOE I.I.K.H. (1986) – *Analytical studies of wave propagation and attenuation*. Geotechnical report n. GR86-15, Civil Engineering Department, University of Texas at Austin.

SUKOLRAT J. (2007) – *Structure and destructuration of Bothkennar clay*. PhD Thesis, University of Bristol.

VIGGIANI G. (1992) – *Small strain stiffness of fine grained soils*. PhD Thesis, City University.

VIGGIANI G., ATKINSON J.H. (1995) – *Interpretation of bender element tests.* Géotechnique, 45, n. 1, pp. 149-154.

Confronto tra le misurazioni delle velocità delle onde di taglio in provini di argilla tenera usando tecniche nel dominio del tempo e della frequenza

Sommario

I bender elements sono stati impiegati per determinare la velocità delle onde di taglio in provini di argilla tenera di Bothkennar usando due differenti tecniche. Le prove sono state eseguite in una cella triassiale a percorso di carico controllato, equipaggiata con bender elements nelle tre direzioni ortogonali, permettendo così di determinare l'anisotropia del materiale a piccole deformazioni. Oltre alla comune tecnica del primo arrivo, si sono impiegati i metodi del ritardo di fase per determinare il tempo di arrivo delle onde. Le letture del ritardo di fase mostrano che i terreni sono dispersivi, il che comporta una variazione delle velocità in funzione delle frequenze. Di maggiore interesse risulta invece l'osservazione secondo cui il metodo nel dominio delle frequenze fornisce con buona affidabilità una stima delle velocità delle onde inferiore rispetto a quella ottenuta con le tradizionali letture nel dominio del tempo. L'articolo descrive le osservazioni fatte su di un provino di argilla naturale di Bothkennar consolidato fino al valore di sforzo di sito e quindi destrutturato mediante l'imposizione di un taglio in condizioni non drenate. Il sistema di acquisizione automatico ha permesso la determinazione delle velocità delle onde di taglio secondo i due metodi durante la prova, che fornisce un utile e non comune insieme di dati. Si confrontano le velocità delle onde e viene analizzata l'evoluzione dell'anisotropia.